

JET-P(92)41

V. Philipps, J. Ehrenberg  
and JET Team

# Analysis of Outgassing after JET Discharges under Beryllium First Wall Conditions

“This document contains JET information in a form not yet suitable for publication. The report has been prepared primarily for discussion and information within the JET Project and the Associations. It must not be quoted in publications or in Abstract Journals. External distribution requires approval from the Publications Officer, JET Joint Undertaking, Abingdon, Oxon, OX14 3EA, UK”.

“Enquiries about Copyright and reproduction should be addressed to the Publications Officer, EFDA, Culham Science Centre, Abingdon, Oxon, OX14 3DB, UK.”

The contents of this preprint and all other JET EFDA Preprints and Conference Papers are available to view online free at [www.iop.org/Jet](http://www.iop.org/Jet). This site has full search facilities and e-mail alert options. The diagrams contained within the PDFs on this site are hyperlinked from the year 1996 onwards.

# Analysis of Outgassing after JET Discharges under Beryllium First Wall Conditions

V. Philipps<sup>1</sup>, J. Ehrenberg  
and JET Team\*

*JET-Joint Undertaking, Culham Science Centre, OX14 3DB, Abingdon, UK*

<sup>1</sup>*Institut für Plasmaphysik, Forschungszentrum Jülich, Germany*  
\* *See Annex*

Preprint of Paper to be submitted for publication in  
Journal of Vacuum Science & Technology



# Analysis of Outgassing after JET-Discharges under Beryllium First

## Wall Conditions

V.Philipps\* and J.Ehrenberg

JET Joint Undertaking, Abingdon, Oxon, OX14, 3EA, UK

\*Permanent address: Institut für Plasmaphysik, Forschungszentrum Jülich, Germany

### Abstract

During the beryllium phase of JET, hydrogen ( $H_2$ , HD,  $D_2$ ), hydrocarbon ( $C_xH_y$ ) and CO outgassing after discharges has been analysed by means of mass spectroscopy and penning gauges. The analysis has been performed over a period of up to 3000 seconds after ohmic and additionally heated limiter and X-point discharges. It has been found that the temporal behaviour of hydrogenic outgassing could be characterized by a uniform power law  $t^{-n}$  with  $n=0.73 \pm 0.1$  which is independent of plasma operation parameters. This result is discussed in view of possible transport and retention mechanisms in and deuterium release mechanisms from plasma facing surfaces. It is concluded that not a single but several mechanisms can explain the release behaviour. However, one of the most plausible explanations is accumulation of hydrogen in limiters and walls. Outgassing of hydrocarbon and CO were significantly lower under Beryllium wall conditions as compared to the earlier all carbon wall conditions

### Introduction

Control of the plasma density in tokamak discharges depends strongly on the hydrogen recycling behaviour of the plasma facing materials. Low H-recycling behaviour of the first wall is an essential requirement to enable effective density control. With carbon or carbonized materials facing the plasma, density control in tokamaks is difficult to achieve [1,2]: energetic particles implanted into surface near regions ( $< 10\text{nm}$ ) are trapped leading within one or after a few plasma discharges to carbon layers saturated with hydrogen (0.4 H/C at R.T./3 /). Under certain conditions this trapped

hydrogen can be liberated in subsequent discharges contributing to an uncontrolled density rise. However, even under conditions of saturation, a large fraction of the hydrogen (up to 90%) admitted into the torus does not appear in the plasma but is retained in the walls or limiters. Therefore the carbon surfaces exhibit a kind of dynamic retention of hydrogen. This is corroborated by results that outgassing of hydrogen is observed from walls and limiter after the end of the discharge. Recently it has been observed in a laboratory experiment that dynamic retention of hydrogen in carbon can be caused by contamination of the carbon surface with metals, a situation always present in tokamaks /4/.

Density control by wall pumping in JET has been altered by the introduction of Beryllium. Beryllium was first dispersed by means of evaporation thereby forming a beryllium layer on the carbon surfaces of limiters and walls and later additionally solid beryllium tiles were used for the limiter and X-point target plates. As a result of this the wall memory effect has been reduced and dynamic retention has been enhanced. There is now almost continuous deuterium pumping throughout a discharge and therefore good density control. To achieve a certain electron density about a factor of four more deuterium gas is needed than before. This partly due to a decrease of the plasma dilution due to a reduction of both the Z of impurities and the impurity concentration but mainly due to increased dynamic retention of deuterium in the material surfaces. The global recycling coefficient can now routinely be less than about 0.9 compared to 0.99 beforehand under all carbon conditions. The larger proportion of dynamically retained hydrogen is also indicated by the larger proportion of outgassing after the discharge (typically a factor of two more compared to the all carbon conditions /5/)

Hydrogen retention in and release from Beryllium has also been investigated independently in laboratory experiments /6,7,8/. When applied to recycling conditions in JET the reported coefficients for diffusion and recombination of deuterium in Beryllium, however, would not allow significant retention of hydrogen in material surfaces. They differ by more than one order of magnitude from similar values derived from global discharge data in JET /9/ suggesting that the surface conditions in JET are different from those in laboratory experiments which as such is not surprising.

In this paper deuterium retention and release is studied by examining the deuterium outgassing after a plasma discharge. In addition the impurity outgassing with beryllium walls has also been analysed and compared with the all carbon wall condition. This gives additional global information on the impurity situation with beryllium walls compared with all carbon wall conditions.

## 2. Experimental

Outgassing of neutrals has been investigated by a set of different penning gauges measuring the evolution of the total pressure after the discharges at four different locations inside the torus. In addition, conventional quadrupole mass-spectrometers (Balzers QMG 102) have been used to analyse the partial pressure of various components. Deuterium gas puffs into the torus without plasma discharges have been used to calibrate deuterium mass spectrometer signals with respect to the total pressure and to determine the background signals at mass 3 and mass 2 (shown in fig 1). The background at mass 2 is mainly caused by cracking of  $D_2$  into  $D^+$  and that at mass 3 by interaction of atomic deuterium with hydrogen at the nearby walls of the ion source of the mass-spectrometer or by HD contamination of the external gas supply itself. At mass 2, background signals between 3 and 5% of the mass 4 signal have been observed. To evaluate the hydrogen (mass 2) outgassing a background value of 5% from mass 4 has been subtracted from signals at mass 2. In the dry runs the mass 3 (HD) fraction increases from about 1% at high  $D_2$  pressures ( $10^{-4}$  mbar) to about 4% at low pressures ( $10^{-6}$  mbar) and thus is not proportional to the  $D_2$  pressure. For this analysis a constant value of 2% has been used for the correction of HD signals.

For other masses spectrometer sensitivities relative to deuterium have been used as given by the mass-spectrometer manufacturer. No attempt has been made to evaluate absolute amounts of outgassing. This has been done before and is published elsewhere [5].

## 3. Results

### 3.1 Outgassing of $H_2$ , HD and $D_2$

After discharges fueled with deuterium under Be conditions, the outgassing neutrals consist nearly totally of  $D_2$  (mass 4), HD (mass 3) and  $H_2$  (mass 2) molecules. The amount of impurity molecules outgassed within 1000 sec after the discharge is less than 1-2% of the hydrogenic component (chapter 3.4). Figure 1 compares the temporal evolution of the mass signals of hydrogenic components after a dry run with those after a plasma discharge in deuterium. If the corrections for

masses 2 and 3 as discussed above are applied the temporal behaviour of mass 2 becomes essentially independent of time, with a remaining intensity similar to the background before the shot. The temporal dependence of the corrected mass 3 signal remains similar to that of mass 4 and it is still substantially larger than in the dry run. The fraction of outgassing of HD depends on the operational history of the tokamak. About 30 deuterium discharges after resumption of operation after venting the torus the HD outgassing was measured to be about 22% of the D<sub>2</sub> release which then decreases only slightly to about 15% after 300 deuterium shots. Even after long term deuterium operation values of about 4% HD outgassing have been measured. From the measured total and partial pressures the outgassing rates as a function of time have been derived according to:

$$Q(t) = (dp(t)/dt \cdot V + p \cdot s) \cdot 273/T_w \cdot 2.62e22 \quad (\text{molecules/sec}) \quad (1)$$

where  $p(t)$  is the pressure (mbar),  $V$  is the JET torus Volume (200m<sup>3</sup>),  $s$  the pumping speed of the pumping system (8 m<sup>3</sup>/sec) and  $T_w$  is the wall temperature at the ion gauges (K). As an example, fig 2 shows the total pressure evolution (a) and the outgassing rate evaluated from it for a soft landed limiter discharge on a long term (b) and a short term (c) time scale. The gas pressure rises sharply when the neutrals which recycle at the limiter and walls cease to be ionised because of the disappearing plasma. This happens very close to the end ( $t=t_e$ ) of the plasma discharge where the plasma current approaches zero. The peak outgassing rate of deuterium just at the end of the plasma discharge ( $t=t_e=24\text{sec}$ ) is about  $2.2 \times 10^{20}$  D-atoms/sec. This value is a lower limit due to the final time resolution (1s) of the pressure gauges but is within the range of the total recycling flux estimated from  $H_\alpha$ -fluxes measured during the ramp down and extrapolated to  $t=t_e$ .

Fig 3 shows the time dependence of the release rate of the total outgassing in a log-log plot. The release rate,  $F_d(t)$ , can be remarkably well represented by a power law according to

$$F_d(t) \propto t^{-n} \quad \text{with } n = (0.73 \pm 0.2) \quad (2)$$

This power law is valid for D<sub>2</sub> and HD outgassing and is maintained about from the beginning of the outgassing (=end of the discharge) until at least 3000 sec after the discharge ( for  $t < 10$  sec the time



resolution of the pressure measurements, gives rise to deviations from the straight line, see fig 3). No obvious change of this power law could be found with changing operational conditions, such as plasma density, current, heating, configuration (X-point or limiter discharge) etc. Also no difference could be observed between the outgassing after the first discharge of the day where the walls could be assumed to be more depleted of deuterium due to overnight outgassing and subsequent shots where the walls are getting progressively loaded with deuterium (However the total background pressure in the torus rises throughout a day with discharges).

### 3.2 Outgassing of impurity gases

Table 1 shows the fraction of non-hydrogenic species which outgasses relative to the  $D_2$  within 1000 s after JET discharges under beryllium wall conditions. Also shown are results of earlier studies in JET by gas chromatography /10 / for both Beryllium and Carbon wall conditions. For comparison, results from similar studies in TEXTOR under carbon conditions are also listed.

Device:	JET (Be/C)		JET (C)	TEXTOR (C)
reference:	this work	/10 /	/10 /	/11/
Hydrocarbons:				
C <sub>1</sub> -type:	$(0.3-1) \times 10^{-2}$	$1 \times 10^{-2}$	$3 \times 10^{-2}$	$(3-7) \times 10^{-2}$
C <sub>2</sub> -type:	$(0.4-2) \times 10^{-3}$			$(0.5-2) \times 10^{-2}$
CO:	$< 5 \times 10^{-4}$	$1 \times 10^{-3}$	$(1-8) \times 10^{-2}$	$(4-12) \times 10^{-2}$

Under Beryllium wall conditions the amount of CO outgassing has been drastically decreased. The reduction is by a factor of about 100 and CO is almost negligible. This is a result of the gettering of

Oxygen by Beryllium which also manifest itself by low Oxygen concentrations in the plasma discharges.

Hydrocarbon outgassing is reduced by about a factor of 3-5 compared to carbon wall conditions. The reduction is also maintained when the plasma interacts with carbon target plates (discharges with X-point at top of the machine) instead with a Beryllium limiter. This is consistent with laboratory results/13/ showing that a small percentage of metallic contaminants on a Carbon surface decreases the hydrocarbon formation. The lower outgassing of carbon containing components after the discharges indicates that CO and hydrocarbon formation is also reduced during the discharge and thus contributes to the lower Carbon concentration in plasmas under beryllium conditions /12/.

#### 4. Discussion

The discussion concentrates on the outgassing phenomena observed for the hydrogenic components. The aim is to find possible hydrogen release mechanism which take place at limiter and walls and which are responsible for the outgassing behaviour and are consistent with the observed recycling during the discharges.

It is observed that at the end of a discharge with soft current landing the plasma density has disappeared and that the neutral gas pressure is still below  $10^{-6}$  mbar. This shows that all the hydrogenic particles introduced by external means are retained in the walls. Assuming that the total gas is either uniformly distributed over the JET limiter or the total wall area an average areal density of  $10^{21}$ - $10^{22}$  or  $10^{20}$ - $10^{21}$  atoms/m<sup>2</sup>, respectively, would be expected. Unfortunately, little is known on the actual distribution of hydrogen between the limiter/target plates and walls. This ratio is determined by the distribution of fluxes and by a possible flux dependence of the hydrogen retention capability of these surfaces. H<sub>α</sub> intensity measurements performed during the plasma current flat top in limiter discharges show that at low densities ( $1 \times 10^{19}$  m<sup>-3</sup>) the limiter to wall flux ratio is about 1:1 rising up to 5:1 at higher densities ( $3 \times 10^{19}$  m<sup>-3</sup>) /14/. During the current ramp down phase, however, this ratio decreases, indicating an increased transfer of particles into the walls. We have to keep in mind that surface area effects can well influence the release process and that an analysis of the global outgassing can only represent an average of the combined effect of all surface areas.

#### 4.1. Outgassing of H<sub>2</sub>, HD, D<sub>2</sub> molecules

The amount of outgassing of HD after plasma discharges is large compared to that in deuterium dry runs only (see fig1), showing that HD is formed by interaction of the plasma with the plasma facing surfaces. It is important to note that the HD release rate follows the same power law as that of D<sub>2</sub>. From this we conclude that the HD is formed predominantly by recombination of hydrogen and deuterium both implanted into the material surfaces due to plasma operation. A process by which the implanted deuterium recombines with residual hydrogen already incorporated in the material would result in a release rate falling off slower for HD than for D<sub>2</sub>.

The H<sub>2</sub>-partial pressure constitutes a continuous background pressure and can dominate the total outgassing at times up to several hours after the end of plasma operation. Therefore it does obviously not originate from surfaces loaded with hydrogen by plasma operation. Hydrogen implanted by plasma operation outgasses completely as HD as expected from the kinetic of the recombination process with hydrogen being the minority component.

#### 4.2. Time dependence of deuterium outgassing

The most striking result is the unique time dependence of the deuterium outgassing which over at least 3000 sec after the discharge can be represented by a power law  $t^{-n}$  with  $n=0.73\pm 0.2$ . Similar power laws have been reported for outgassing in ASDEX /15/ and TFTR /16/ and are usually also observed during pumping down of a non baked vacuum system or during glow and/or RF discharge cleaning procedures of large vessels/17,18/. In these cases typical values for the exponent  $n$  are around 1. The temporal dependencies have been explained in terms of long range diffusion processes from the interior of a solid material uniformly loaded with hydrogen. In this case a  $t^{-0.5}$  dependence of the outgassing flux is expected /19/.

In a tokamak discharge the loading of material surfaces with deuterium is normally quite different: the solid is loaded with deuterium for only a few seconds (the duration of the discharge) followed by long time outgassing between discharges. On erosion dominated areas the loading leads to a non-uniform

near-surface concentration profile which is peaked near the surface ( $< 10\text{nm}$ ). A more uniform distribution might be created on deposition dominated regions by simultaneous deposition of Carbon or Beryllium with deuterium forming a layer of C/Be quasi uniformly loaded with deuterium (so called co-deposition /20/). Provided that the escape rate of deuterium from these layers is less than the growth rate of it the release after the end of the discharge might indeed be similar to that from a uniformly loaded bulk material. The total release of deuterium could well be affected by the existence of different implantation profiles in different surface areas of limiters and walls.

The release process itself could be caused by a variety of different possible mechanisms. These mechanisms are listed below and classified in the usual way as initially proposed by Doyle /21/. (i) thermal detrapping from traps, (ii) diffusion through the surface and into the bulk (DD process), (iii) recombinative release at the plasma facing surface as well as at the rear surface of the limiter or wall (RR process), (iv) diffusion into the bulk and recombination at the surface (RD process). First the outgassing is discussed on the basis that the material has been loaded during one single discharge and later we discuss the influence of a residual H/D background concentration in the material which can be expected to be present due to incomplete outgassing in between shots. Analytical approximations of the outgassing can be obtained for some simple cases. For other cases, however, numerical methods are needed. Therefore a code has been developed (similar to that described in /22/) which computes the global recycling of hydrogen during the discharge and the outgassing afterwards in a selfconsistent manner. The main elements of it are: the plasma particle balance equation is solved with the plasma loss term being the particle source term for the diffusion equation describing particle transport within the material surfaces. Two surfaces of identical properties are assumed and the respective share of fluxes they receive from the plasma is prescribed by a flux branching coefficient. The recycling flux feeding the plasma from these surfaces is governed by recombination of atomic deuterium into molecules. Free parameters are: the diffusion and recombination coefficients, the surface areas of the material surfaces, the global plasma particle confinement time and the flux branching coefficient. Possible diffusion and recombination coefficients are derived from JET discharges as has been shown in /9/. Surface areas come from the JET geometry and particle confinement times and the total flux branching are derived from density and  $H_{\alpha}$  flux measurements /14/. The loading of walls and limiters has been simulated using a discharge duration of 22 sec assuming a linearly increasing particle confinement time from 0 s to 0.4

s (the latter value being a typical particle confinement time for JET limiter discharges with a plasma current of 3 MA) in the current ramp up phase and a branching coefficient (ratio of limiter to wall flux) linearly increasing from 0 to 0.9. From 4 to 18sec of the discharge these parameters are kept constant whilst during the ramp down phase from 18 to 22 sec they are changed in a fashion symmetric to the ramp up phase. For the gas input experimental values are used. Validation of the parameters is performed by comparing the theoretical density, pumping and fuelling evolution during the discharge and the outgassing afterwards with the corresponding experimental results.

### 4.3 Analysis of the outgassing of deuterium deposited in a single discharge

#### 4.3.1 Detrapping controlled release

If the release of particles from materials is controlled by thermal detrapping from one kind of trap sites the release rate decreases exponentially with time, in contrast to the experimental observation. Thus, to explain the observed outgassing by such a process we have in addition to assume that the overall outgassing is determined by release from a distribution of trap sites with a suitable distribution of trap binding energies.

#### 4.3.2. Diffusion controlled release process

For diffusion controlled release on erosion dominated surfaces the deuterium concentration in the near surface region is strongly depth-dependent. For implantation of particles at  $x=R$  into a semi-infinite solid the deuterium concentration  $c_d(x,t)$  is given by :

$$dc_d(x,t)/dt = D d^2c_d/dt^2 + F_d(t) \delta(x-R) \quad (3)$$

with  $D$  the Diffusion coefficient ( $m^2/sec$ ) and  $F_d(t)$  the impinging deuterium flux deposited at the implantation depth  $x=R$  (typically 1-5 nm). After loading the material during the discharge for a time  $t_s$  (typically 10-30sec at JET),  $c_d(x)$  can be approximated by the distribution illustrated in fig 4, curve a: it increases nearly linearly up to  $x=R$  (valid for  $D > R^2/2t_s \approx 5 \times 10^{-17} m^2/sec$ ) and decreases then

exponentially with a half width of  $(D \cdot t_s)^{0.5}$ . From this the deuterium inventory  $I_d(t)$  at the time  $t$  can be approximated using the impinging flux density,  $F_d(t)$ , the mean range  $R$ , the effective overall wall area  $A$ , and the diffusion coefficient  $D$  :

$$I_d(t) = F_d R/D [R/2 + (D t)^{0.5}] A \quad (4)$$

An effective diffusion coefficient of about  $10^{-17} \text{ m}^2/\text{sec}$  is needed to obtain a particle retention similar to that observed in JET of about  $10^{22}$  D-atoms per shot, assuming  $A = 10 \text{ m}^2$ ,  $R = 5 \text{ nm}$ ,  $F_d = 1.6 \times 10^{20} \text{ m}^{-2}\text{s}^{-1}$  and  $t = 10 \text{ sec}$ . This value of the diffusion coefficient is about 5 orders of magnitude smaller than that reported for pure beryllium(8). The JET first wall, however, consists of a mixture of Carbon/Beryllium material with a diffusion coefficient possibly completely different to that of pure beryllium. Effective tritium diffusion in Berylliumoxyd at 500 K was measured to be  $3 \times 10^{-29} \text{ m}^2/\text{sec}$  /23/, 14 orders of magnitude smaller than for pure Beryllium.

After loading the release rate  $F_d(t)$  at the near surface is given by

$$F_d(t) = \int_x c_d(x) \frac{1}{4} \pi D^{-0.5} t^{-1.5} \cdot \exp(-x^2/4 D t) dx \quad (5)$$

The exponential term in equation 3 approaches gradually unity for times  $t > t_s$  (the loading time during the discharge) and the outgassing flux approaches then a  $t^{-1.5}$  dependence on time. In a log-log plot of the outgassing rate with time the diffusion controlled outgassing calculated for  $D = 10^{-17} \text{ m}^2/\text{sec}$ , a loading (discharge) time of 12 sec and an implantation depth of 2 nm is compared in Fig 5 with the experimental result. The time dependences are clearly different.

The situation changes if we assume diffusive outgassing from deposition regions. There we might assume a uniform deuterium concentration throughout the deposited layer as described above. The diffusive release on the front surface from a uniformly loaded layer with simultaneous diffusion into the underlying material follows a  $t^{-0.5}$  time dependence for fairly long period of times (the length of this period is given approximatly by  $t = 0.1 d^2/D$ , with  $d$  the thickness of the layer and  $D$  the diffusion constant) before it turns gradually to a  $t^{-1.5}$  dependence.

In order to apply successfully the "layer model" to JET outgassing we have to assume that diffusion into the underlying material is prevented. This might be caused by internal surfaces at

which recombination occurs or by an internal diffusion barrier. However we have to keep in mind that in any case the diffusion coefficient has to be below  $10^{-17} \text{ m}^2/\text{s}$ . During the discharge this low mobility would cause mobile hydrogen concentrations of some  $10^{28} \text{ atoms/m}^3$ , a value near the solid state concentration of the host material.

#### 4.3.3. Recombination controlled release

For this process (RR) the release kinetics would not be different in erosion or deposition regions. For this situation the deuterium diffusion must be either very fast (the concentration profile remains always flat) or negligible small in which case the deuterium occupies only surface near sites however at a large local concentrations. The release flux  $F_d(t)$  is given by:

$$F_d(t) = K \cdot c_d(t)^2_{(x=0)} \quad (6)$$

with  $K$  a recombination rate ( $\text{m}^4/\text{sec}$ ) and  $c_d(x=0)$  the deuterium concentration at the surface. The time dependence of  $F_d(t)$  can be given analytically:

$$F_d(t) = \alpha / (\alpha t + N_0)^2 \quad (7)$$

with  $\alpha = K/(A d^2)$ ,  $A$  the loaded area ( $\text{m}^2$ ) and  $d$  (m) the thickness over which the deuterium is uniformly distributed, which is either the thickness of the wall (diffusion very fast), or, for  $D$  negligible small, the "thickness" of a surface layer with surface related sites (roughly one monolayer).  $N_0$  is the number of deuterium atoms loaded onto the area  $A$ . It follows that, for times  $t \gg (A d^2)/(K N_0)$ ,  $F_d$  decreases with  $t^{-2}$ . For decreasing times, the time dependence gradually weakens. In an example this is demonstrated in Fig 5, where the release of  $10^{22}$  deuterium atoms distributed over an area of  $7 \times 10^2 \text{ m}^2$  (possibly the limiter) (curve a) and of  $4 \times 10^{21}$  deuterium distributed over  $2 \times 10^2 \text{ m}^2$  (possibly the wall) (curve b) is shown in a log-log plot. The time dependence of the initial release is flat increasing then gradually to a  $t^{-2}$  dependence. The onset of this change depends on the deuterium concentration and the value of  $K$ . In the example shown in Fig 5 the deuterium was assumed to be retained in surface related sites only (an infinite small diffusion) which needs a small recombination

coefficient ( $10^{-35} \text{ m}^4/\text{s}$ ) in order to reduce the release rate to values comparable with the experimentally observed ones (indicated by the dashed line in fig5). If only one single area is loaded uniformly with deuterium ,no uniform power law can be obtained. However if areas of different sizes are loaded with different deuterium concentrations,the resulting overall release rate tends to obey a more uniform power law (adding curve a and b). Thus,with these assumptions, a RR-determined release process could be constructed such that it is similar to the experimental time dependence. At any rate one has either to assume a very fast diffusion processes in combination with a large recombination coefficient ( $> 10^{-28} \text{ m}^4/\text{sec}$ , depending on d) or a negligible small diffusion coefficient in combination with a small recombination coefficient (about  $10^{-35} \text{ m}^4/\text{sec}$ ). These values are not in agreement with measurements of the diffusion coefficient /8/ or recombination coefficient /6,7/ on beryllium. However,as said before they might not be relevant for JET with its beryllium/carbon surface /24/

#### 4.3.4. Recombination-diffusion controlled release

If deuterium release is determined by both recombination on the surface as well as by diffusive transport into the bulk material the deuterium concentration after loading would be qualitatively like that shown in Fig 4b. The desorbing flux is then still given by equation 4 but the flux from the surface is balanced by a corresponding diffusive flux from the bulk arriving at the surface .

$$F_d(t) = K c_d^2(t)_{(x=0)} = -D dc/dx \quad (9)$$

Under these conditions,no analytical solution for the time dependence of the outgassing flux is possible. For an initial and transient time after loading analytical approximations /25,26/ have been developed showing that the flux is determined by:

$$F_d(t) \propto t^{-0.5} \quad (8)$$

and then decreases faster.

More numerical calculations of the RD-determined release have been performed. First, a semi-infinite solid has been assumed with particle loading during only one discharge. The loading is



determined by the waveform for the particle confinement time and by the flux branching between limiter and wall as described in section 4.2. and illustrated in fig 6a. For the calculations the following parameters have been used:  $K=5 \times 10^{-35} \text{ m}^4/\text{sec}$ ,  $D=1 \times 10^{-13} \text{ m}^2/\text{sec}$ , limiter area of  $10 \text{ m}^2$ , wall area  $50 \text{ m}^2$ ). Figure 6b shows the calculated total particle content for the plasma, the limiter and the wall for a particle input waveform as indicated. Also shown is the experimental plasma content. For this example, the slope of the outgassing rate as a function of time is shown in fig 7, curve a. As can be seen, the time dependence of the outgassing flux steepens gradually, starting with an exponent of around 0.5, in agreement with the analytical approximations, and then increases continuously reaching at about 200 sec a value of 1.2 with no further change. No uniform power law in the vicinity of 0.7 for times up to 3000 sec can be obtained whichever combination of D and K is used. Thus the assumption of a single RD-determined release process after single plasma loading of a semi-infinite solid also fails to explain the experimental data. However, if it is assumed that outgassing occurs from a surface layer without losses to the bulk material, thus preventing long range diffusion deep into the material, the slope can be reduced for a fairly long time interval. The variation of the slope with time for this case is given in fig 7, curve b for a layer thickness of  $3 \times 10^{-6} \text{ m}$ . Assuming again a distribution of such layers with different depths a more or less uniform power law could be constructed. The assumption of such a layer will not affect the recycling during the discharge since the backsurface of the layer will be reached only during the long term outgassing. For too thin a layer a RR situation could be created with the release being too fast. For the diffusion coefficient given above the layer thickness is restricted to values of about  $3 \times 10^{-6} \text{ m}$ .

#### 4.4 Evolution of the deuterium outgassing after repeating plasma loading

So far, only outgassing of deuterium deposited in surfaces during a previous discharge has been considered. It is, however, known that outgassing is not complete within the time between two discharges. To simulate the effect of accumulation of deuterium in the surfaces a set of typical discharges with parameters as given in section 4.2. and 4.3.4 have been calculated with outgassing allowed for 600 sec between shots. The residual hydrogen concentration after 600 sec was then taken for the initial hydrogen limiter and wall concentration of for the next discharge. The calculations have been performed for semi-infinite solids for RD and for DD controlled release processes.

For the RD controlled release ( $D=10^{-14} \text{ m}^2/\text{s}$ ,  $K=5 \times 10^{-35} \text{ m}^4/\text{s}$ ,  $R=5\text{nm}$ ) the release fraction after the 1<sup>st</sup> discharge is about 60% of the particle input increasing continuously to about 80% after the 10<sup>th</sup> discharge. Fig 8 shows the release rate as function of time and the slope of it in a log-log plot for the outgassing after the 11<sup>th</sup> discharge. The release can be well approximated by a  $t^{-n}$  power law with  $n=0.85$ .

For the DD-controlled release ( $D=10^{-17} \text{ m}^2/\text{s}$ ) the release fraction for the first discharge is about 90% with a slope of the release rate typical for diffusional release (curve a, fig9). However, after the 21<sup>st</sup> discharge this slope is reduced (curve b, fig9) and after further discharges it is even more. (curve c, fig9). The average slope is then less than 1. The general result that the outgassing rate becomes closer and closer to a unique power law is almost independent of the values for  $D, K, A$  as long as accumulation is allowed. It should also be stressed that the accumulation of deuterium in walls has no significant influence on the wall pumping capacity and thus density evolution during the discharge (neither in DD, nor in RD regime).

Experimentally it was never observed that the outgassing fell faster than with  $t^{-0.70}$ . This indicates that the JET walls have always been loaded with hydrogen starting with conditioning processes.

## Summary

During the beryllium phase of JET the fraction of hydrocarbon outgassing is  $(3-12) \times 10^{-3}$  of the deuterium outgassing independent of plasma operation on beryllium belt limiters or carbon X-point tiles. The fraction of CO outgassing is below  $10^{-3}$  of that of deuterium. Hydrocarbon and CO outgassing have decreased by factors of about 5-10 and more than 100 respectively when compared with fully carbon wall conditions.

The time dependence of the deuterium outgassing after plasma discharges follows a power law of  $t^{-n}$  with  $n=0.73 \pm 0.2$ . This holds for periods of times of at least 3000 sec after a discharge and no dependence of the plasma operation conditions has been detected. The initial release rate of deuterium from surfaces after the end of a discharge is within the range of the recycling rate at the end of the discharge suggesting that the release process with and without plasma is the same. The analysis shows that there is not just one type of deuterium transport and release which could explain

in a consistent manner the recycling during the discharge and the outgassing behaviour after the discharge.

A separation into two groups of likely mechanisms is possible:

**I. Mechanisms where loading of walls and limiters with particles from single discharges is assumed to explain the outgassing.**

For such a case the following conclusions can be drawn:

I.1. For a thermal detrapping release mechanism an appropriate distribution of binding energies (rather than a single binding energy) is needed.

I.2. For a pure recombination controlled process (RR) a negligible small diffusion coefficient in combination with a slow recombination ( $< 10^{-35} \text{ m}^4/\text{s}$ ) or a fast diffusion with a fast recombination ( $> 10^{-28} \text{ m}^4/\text{s}$ ) is needed. In addition a distribution of surface areas loaded with different deuterium concentrations is required.

I.3. For a diffusion controlled process (DD-process) a layer structure for the surface is needed which is uniformly loaded possibly by codeposition of deuterium with Beryllium or carbon. Release can occur either from one or from both surfaces of the layer but particle losses into the bulk material must be prevented. The diffusion coefficient must be less than  $10^{-17} \text{ m}^2/\text{sec}$ .

I.4. For a process controlled by recombination at the surface and by diffusion into the material, (RD-process), a layer structure for the surface has also to be assumed to prevent during the outgassing a too fast fall off of the release rate with time.

**II. Outgassing determined by accumulation of deuterium from previous discharges**

For this case the progressive loading of the material with hydrogen as a consequence of incomplete outgassing gradually develops a  $t^{-n}$  dependence of the release rate with  $n < 1$  regardless of whether the release is DD or RD limited. Increasing wall loading decreases  $n$  gradually from 1 down to 0.5.

We have to note that a final distinction between the different mechanisms mentioned above cannot be made from the global analysis of the outgassing. However from the fact that in tokamaks with different wall conditions (steel walls, carbon, beryllium, boron) the temporal outgassing behaviour seems to be very similar/27/ and that the gas release is normally less than 100% in between discharges a very plausible explanation is that accumulation of deuterium in plasma facing materials plays the dominant role for the temporal outgassing behaviour.

### **Acknowledgement**

We gratefully acknowledge the assistance of the First Wall Group in JET in using the quadrupole mass spectrometers.

## References

- [1] J.Winter, J.Vac Sci Technol. A5, (4), (1987),2286
- [2] J.Ehrenberg,J.Nucl.Mater. 162-164, (1989), 63
- [3] W.R. Wampler ,K.Brice, J.Nucl.Mater., 102, (1981), 304
- [4] C.Jandl, W.Möller, B.Scherzer, 18<sup>th</sup> Europ. Conf.on Control.Fusion and Plasma Physics,3-7 June 1991, Berlin, Europhysics Conference abstracts, Vol 15 C, 245
- [5] R. Satori,G.Saibene,J.Nucl.Mater., 176-177, (1990), 624.
- [6] G.Saibene,R.SatoriR.Satori,J.Nucl.Mater., 176-177, (1990),618
- [7] W.L.Hsu ,R.A.Causey,B.E.Mills et al, J.Nucl.Mater. 176-177, (1990), 218
- [8] P.M.S.Jones,R.Gibson,J.Nucl Mater. 21 (1967) 353 and AWRE report No 0-2/67
- [9] J.Ehrenberg,V.Philipps,L.De Kock, J.Nucl.Mater. 176-177 (1990) 226
- [10] R.Satori,G.Saibene,Jet Report about Workshop on Plasma-surface interactions in JET,June 15 16,1989,
- [11] V.Philipps et al,to be published
- [12] P.Thomas and the JET Team,J.Nucl.Mater., 176-177, (1990), 3
- [13] V.Philipps,K.Flaskamp,E.Vietzke J.Nucl.Mater. 122-123, (1984), 1440
- [14] M.Stamp ,private communication
- [15] W.Poschenrieder,G.Venus J.Nucl.Mater. 111/112, (1982), 29
- [16] F.Dylla,private communication

- [17] B. Dayton, in Transactions of the 8<sup>th</sup> Vacuum Symposium and Proceedings of the 2<sup>nd</sup> International Congress on Vacuum Science and Technology 1961 (Pergamon, New York, 1962), Vol 1, 42
- [18] H.F. Dylla et al, J. Vac. Sci. Technol 15, (1978), 734.
- [19] K. Dimoff et al, J. Vac. Sci. Technol. A 6 (5), (1988), 2876
- [20] R. Behrisch, J. Ehrenberg, M. Wielunski et al, J. Nucl. Mater. 145-147, (1987), 723
- [21] B. Doyle, J. Nucl. Mater. 111/112, (1982), 628
- [22] J. Ehrenberg, S.A. Cohen, L. De Kock et al, 14<sup>th</sup> Europ. Conf. on Control. Fusion and Plasma Physics, Europhysics Conference Abstracts Vol 11d, part II, 706
- [23] J.D. Fowler et al, J. Am. Ceram 60 (3-4), 155
- [24] P. Coad, S. Burch, F. Lama et al J. Nucl. Mater. 176-177, (1990), 145
- [25] P.C. Stangeby J. Nucl. Mater. 126, (1986), 190
- [26] T.J. Dolan, J. Nucl. Mater. 92 (1980), 112
- [27] V. Philipps, J. Ehrenberg, H.G. Esser et al, 18<sup>th</sup> Europ. Conf. on Control. Fusion and Plasma Physics, 3-7 June 1991, Berlin, Europhysics Conference abstracts, Vol 15 C, III, 49

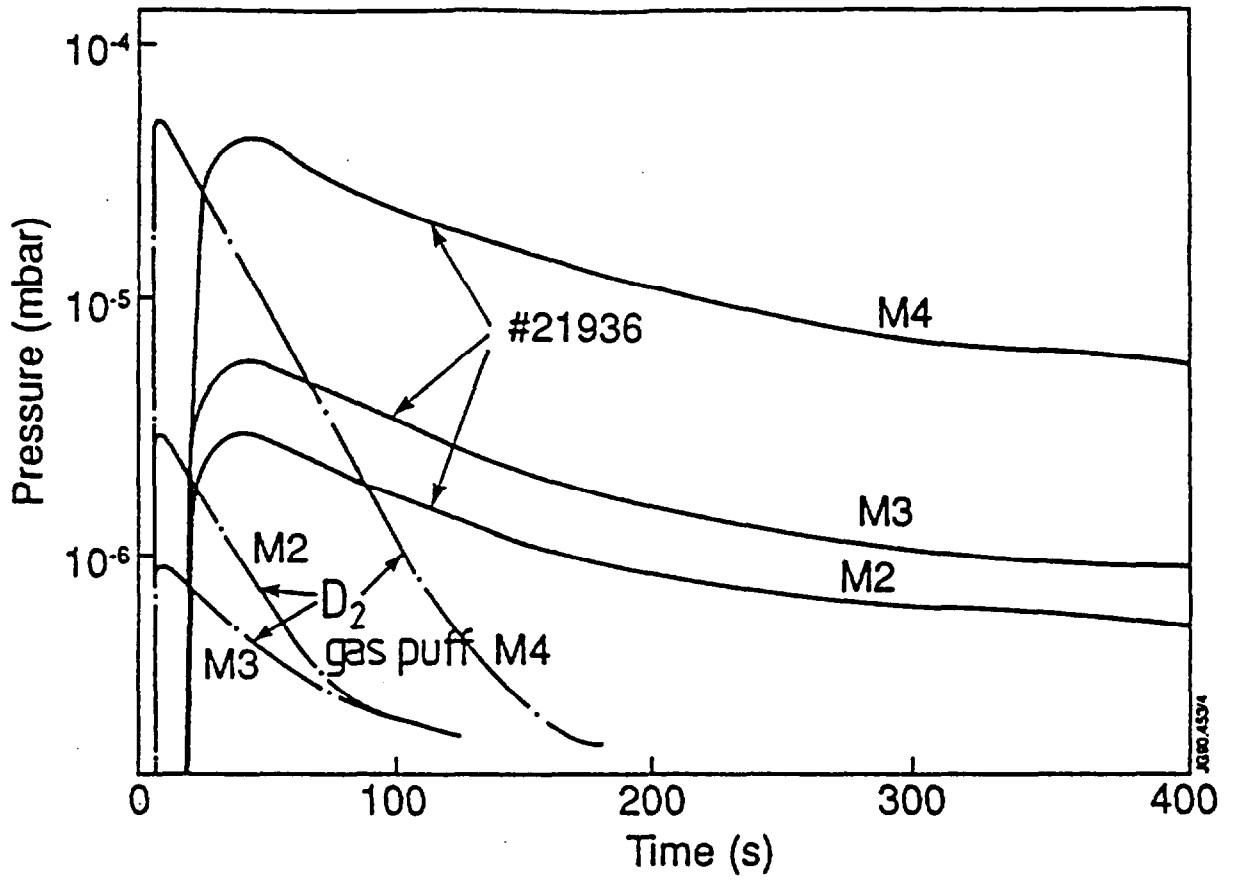


Fig1: Typical time evolution of partial pressures of  $H_2$ , HD and  $D_2$  after a tokamak discharge (shot N<sup>o</sup> 21936) and after a deuterium gas puff only (dashed lines)

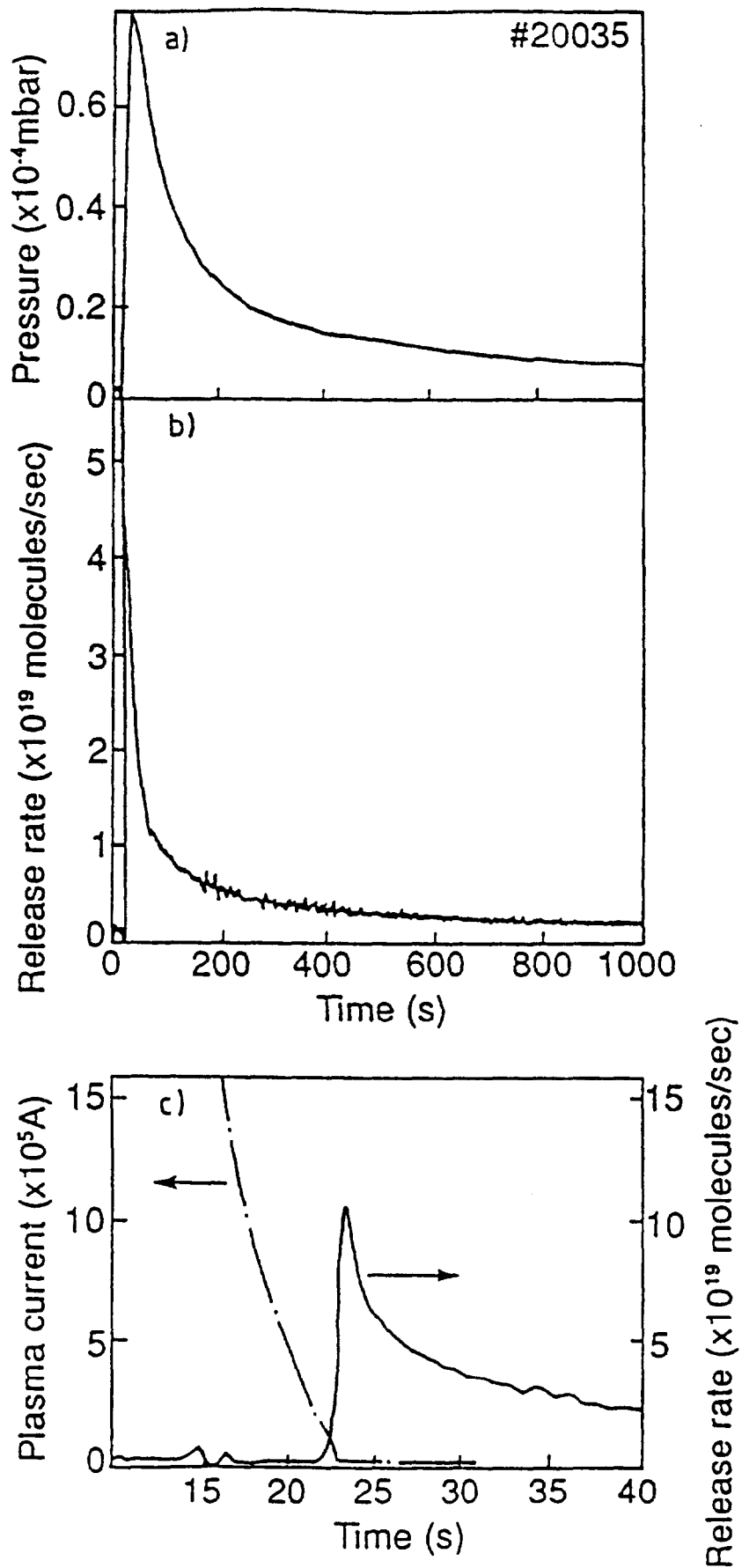


Fig2: Typical total pressure evolution after a discharge under Beryllium wall conditions (a) together with the corresponding outgassing rate on a long time scale (b) and on a short time scale (c). Fig2c shows also the plasma current during plasma ramp down.



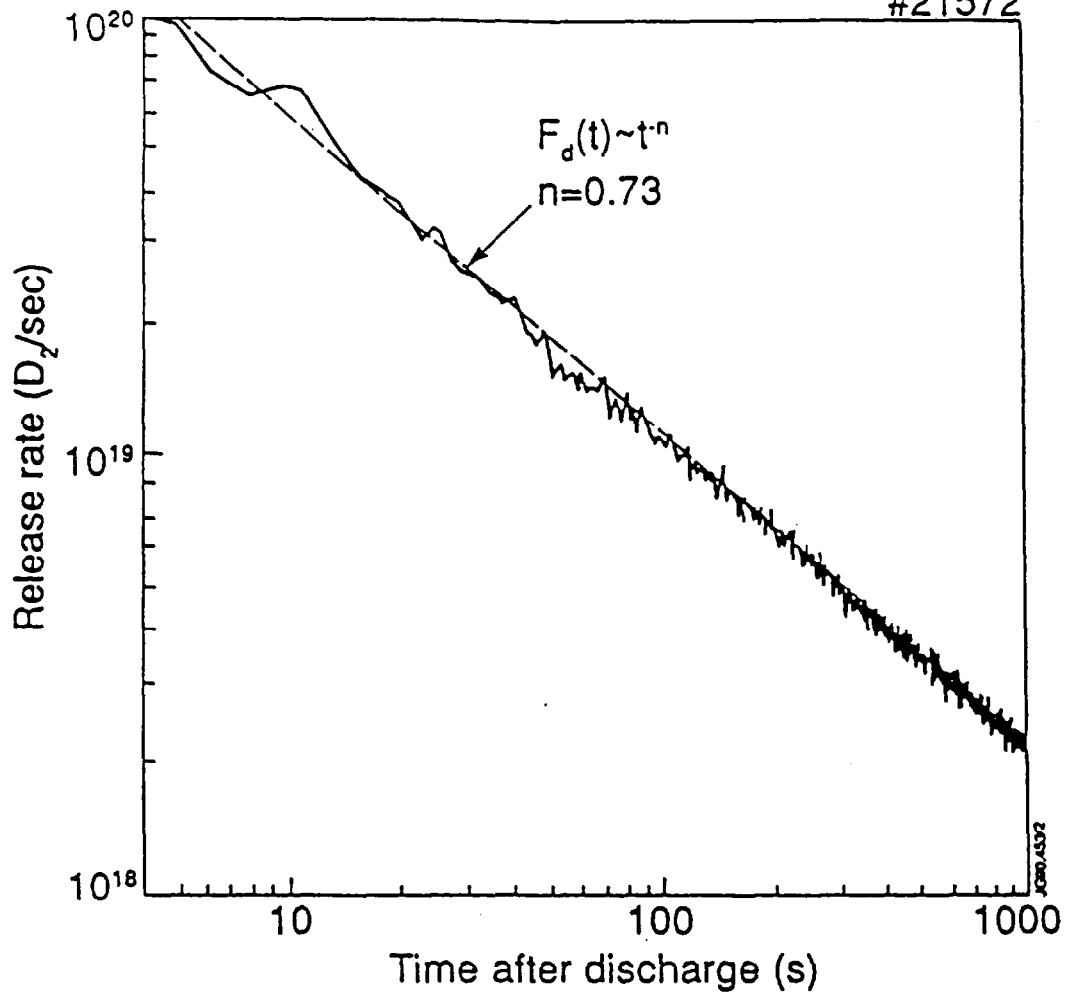


Fig3: Log-log plot of the total outgassing rate versus time

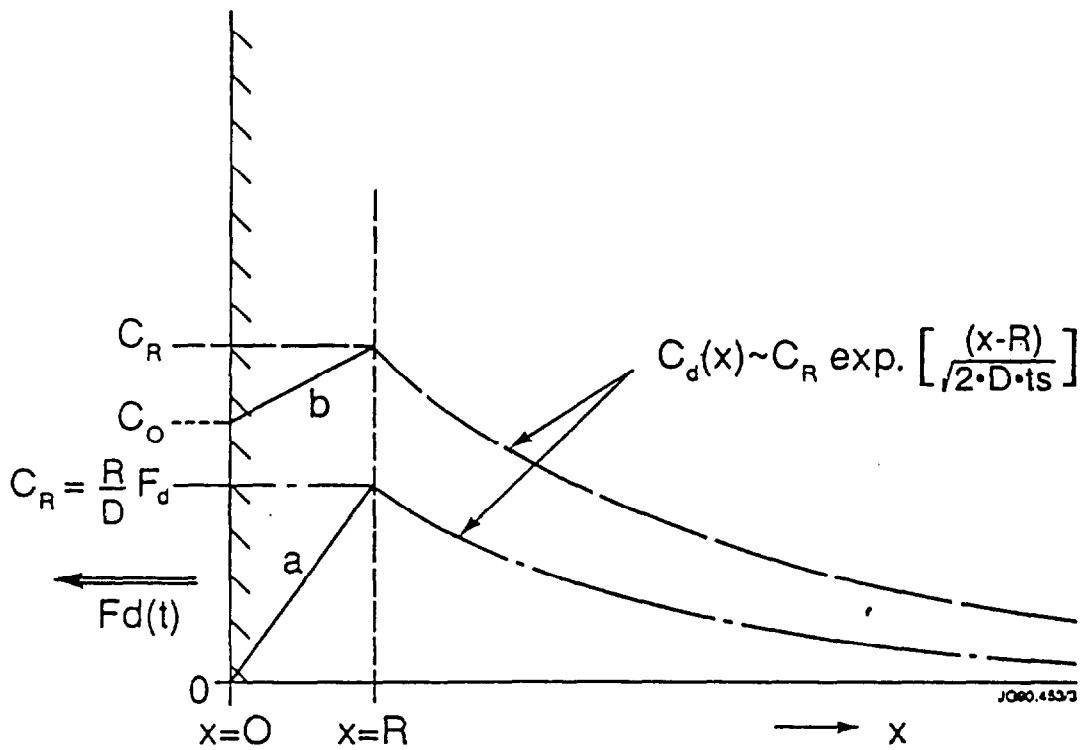


Fig4: Schematic diagram of the near surface deuterium concentration in case of a diffusion controlled process (a) and a diffusion-recombination controlled process (b).

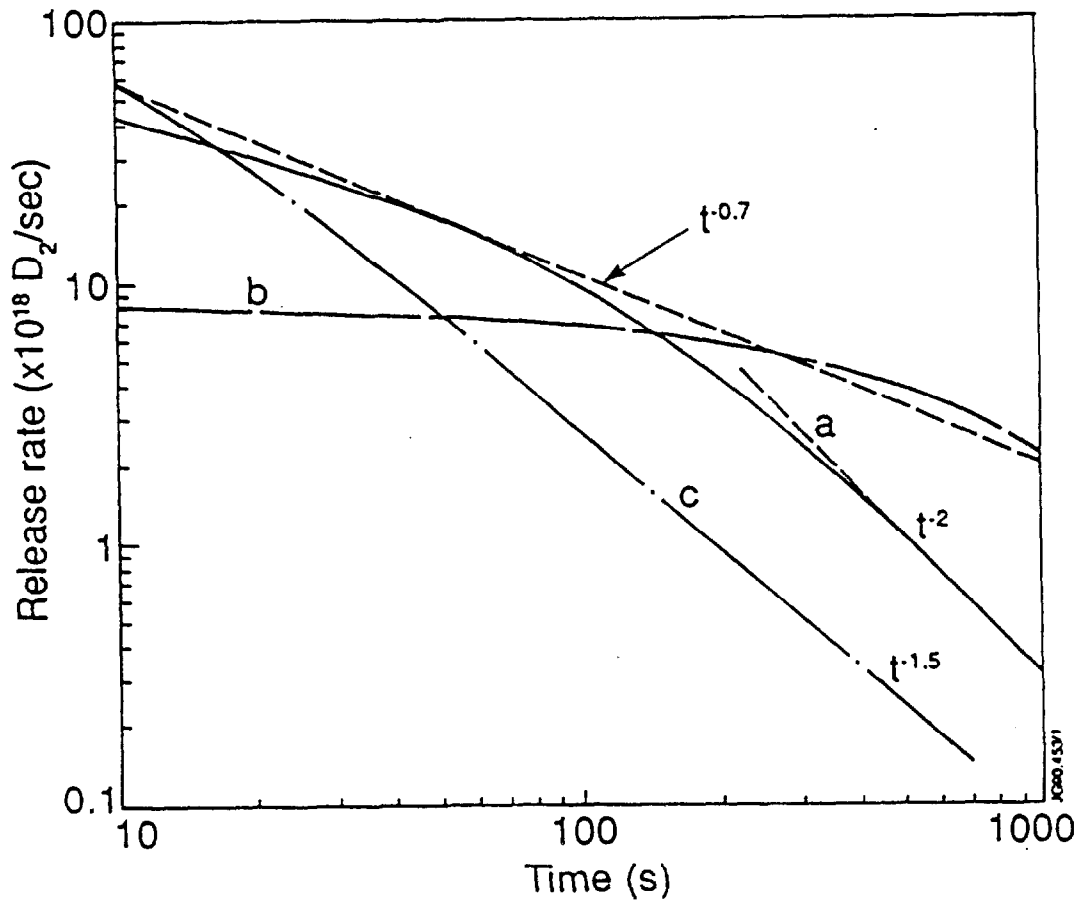


Fig5: Log log plot of the release rate versus time calculated for a recombination limited release process from a small area ( $7 \text{ m}^2$ ) loaded with  $10^{22}$  D-atoms (a) and a larger area ( $200 \text{ m}^2$ ) loaded with  $4 \times 10^{21}$  D-atoms ( $K = 10^{-35} \text{ m}^4/\text{sec}$ ) (b). Curve c shows the release calculated for a diffusion controlled release process alone (range =  $2 \text{ nm}$ ,  $D = 10^{-17} \text{ m}^2/\text{sec}$ ).

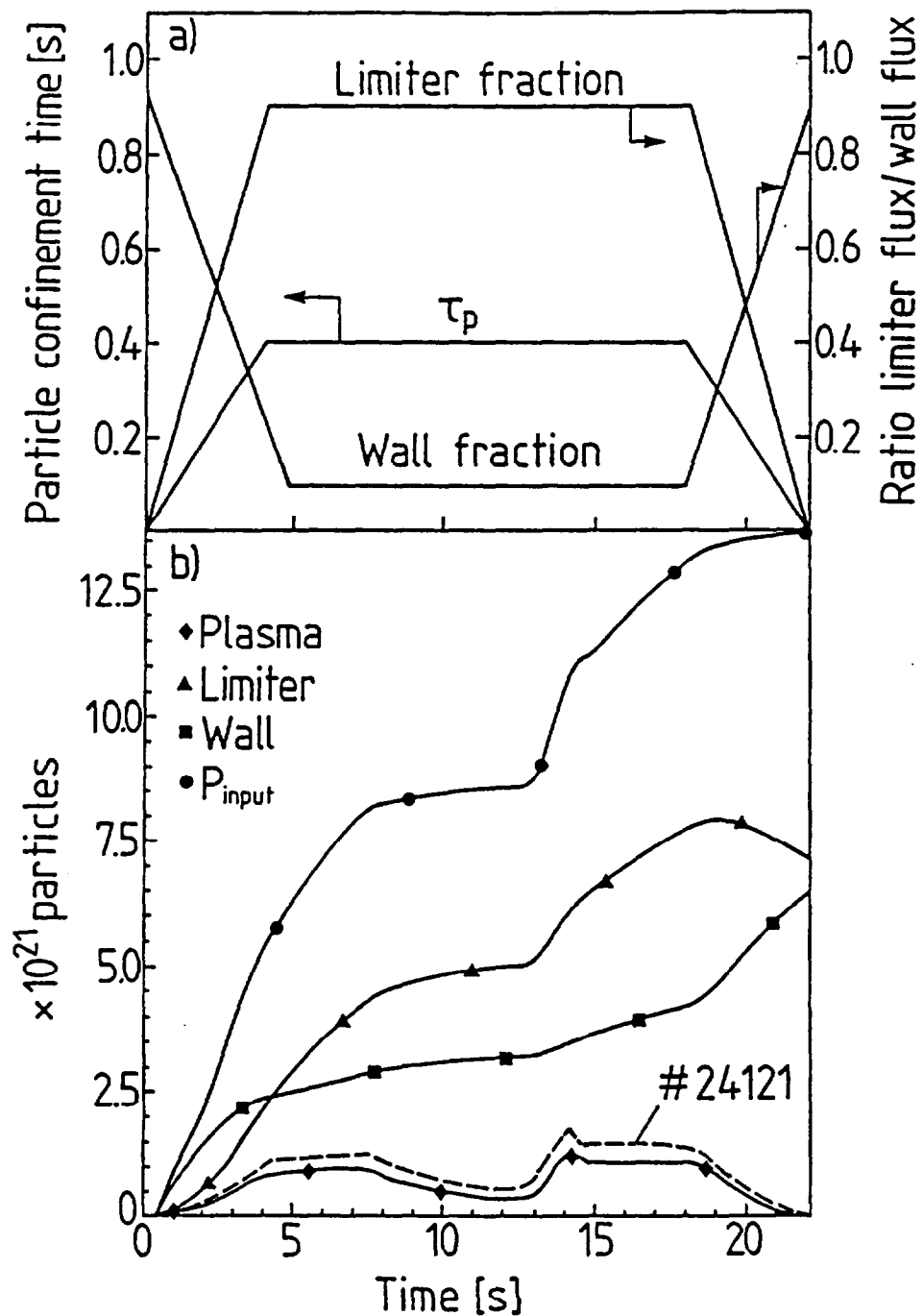


Fig6,a: Model assumptions for the time evolution of the particle confinement time and the flux branching between wall and limiter. b: calculated particle contents in the plasma, wall and limiters using  $K=5 \times 10^{-35} \text{ m}^4/\text{s}$ ,  $D=10^{-14} \text{ m}^2/\text{s}$ , Wall area =  $50 \text{ m}^2$ , limiter area =  $10 \text{ m}^2$  and the experimental total deuterium input for shot 24121. Also indicated is the experimental deuterium plasma content (dashed curve).

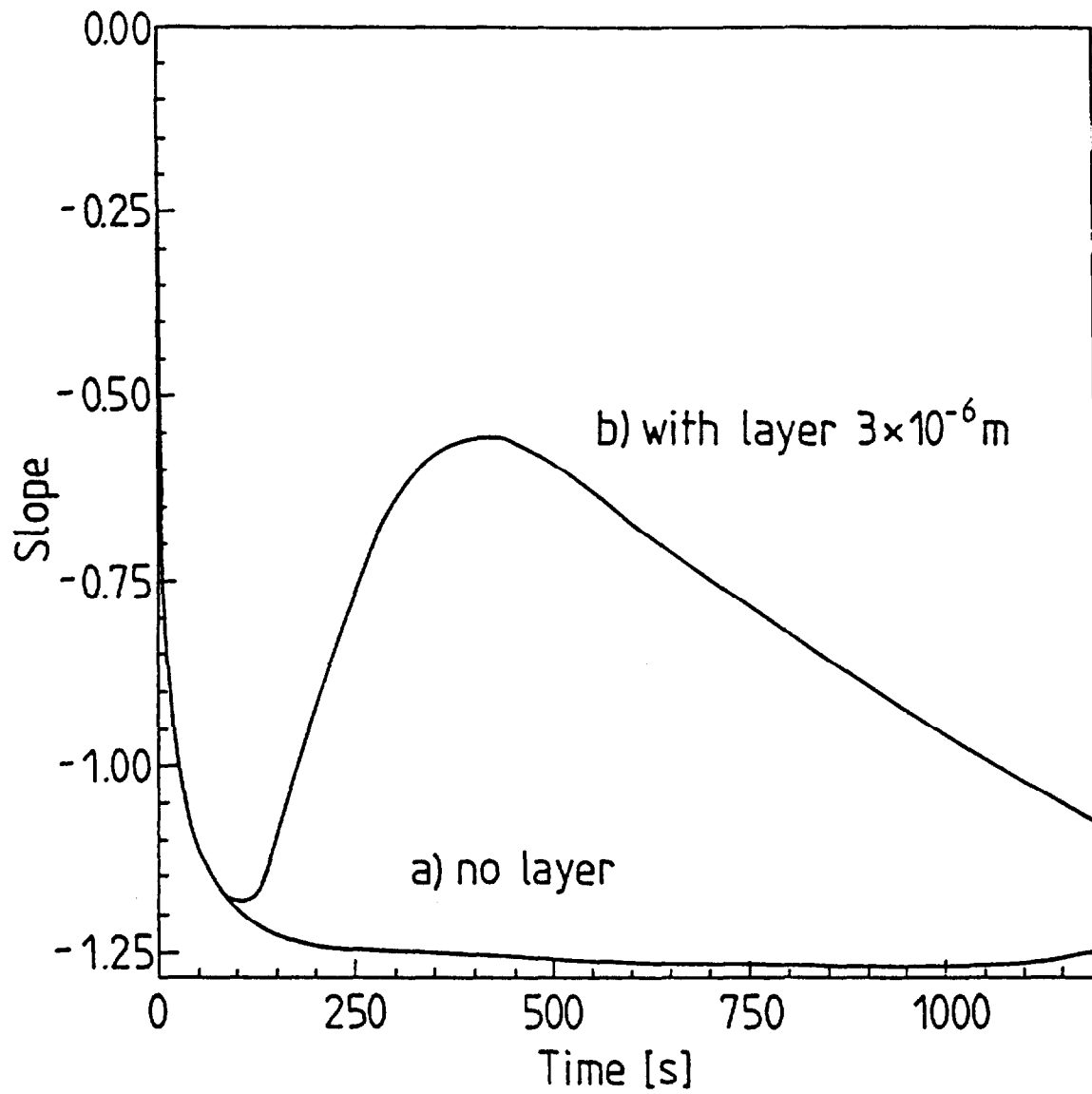


Fig 7: Calculated slopes of the logarithms of the outgassing rates versus logarithm of time for a RD-controlled outgassing process with  $K=5 \times 10^{-35} \text{ m}^4/\text{s}$ ,  $D=10^{-14} \text{ m}^2/\text{s}$ . The figure shows the slope for a semi-infinite solid (a) and for a layer with  $d=3 \times 10^{-4} \text{ cm}$  (b).

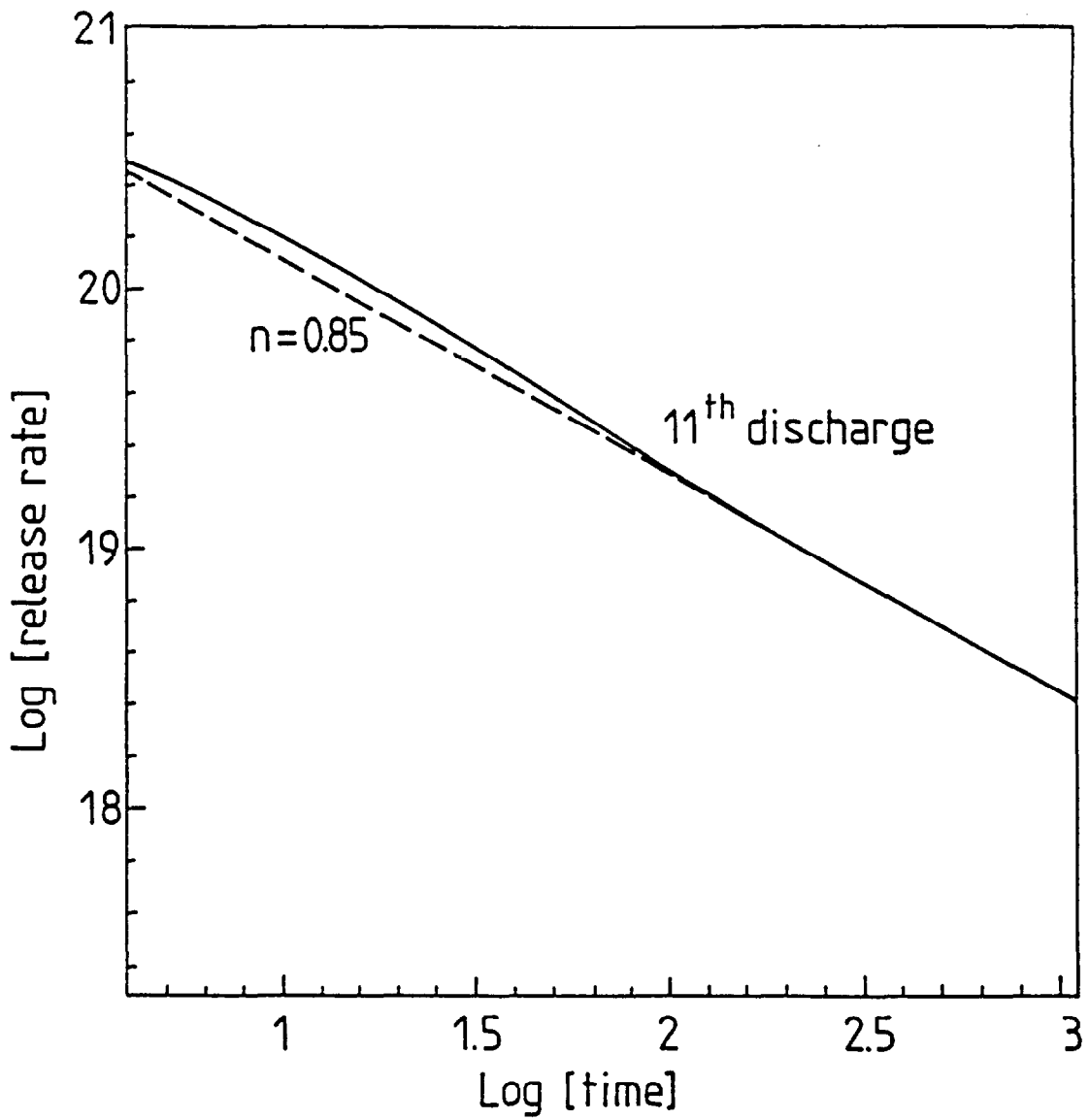


Fig 8: Logarithm of the release rate versus logarithm of time after 11 successive plasma loadings with outgassing for 600 sec between shots for a RD process with  $K=5 \times 10^{-35} \text{ m}^4/\text{s}$ ,  $D=10^{-14} \text{ m}^2/\text{s}$  and  $R=5 \text{ nm}$ .

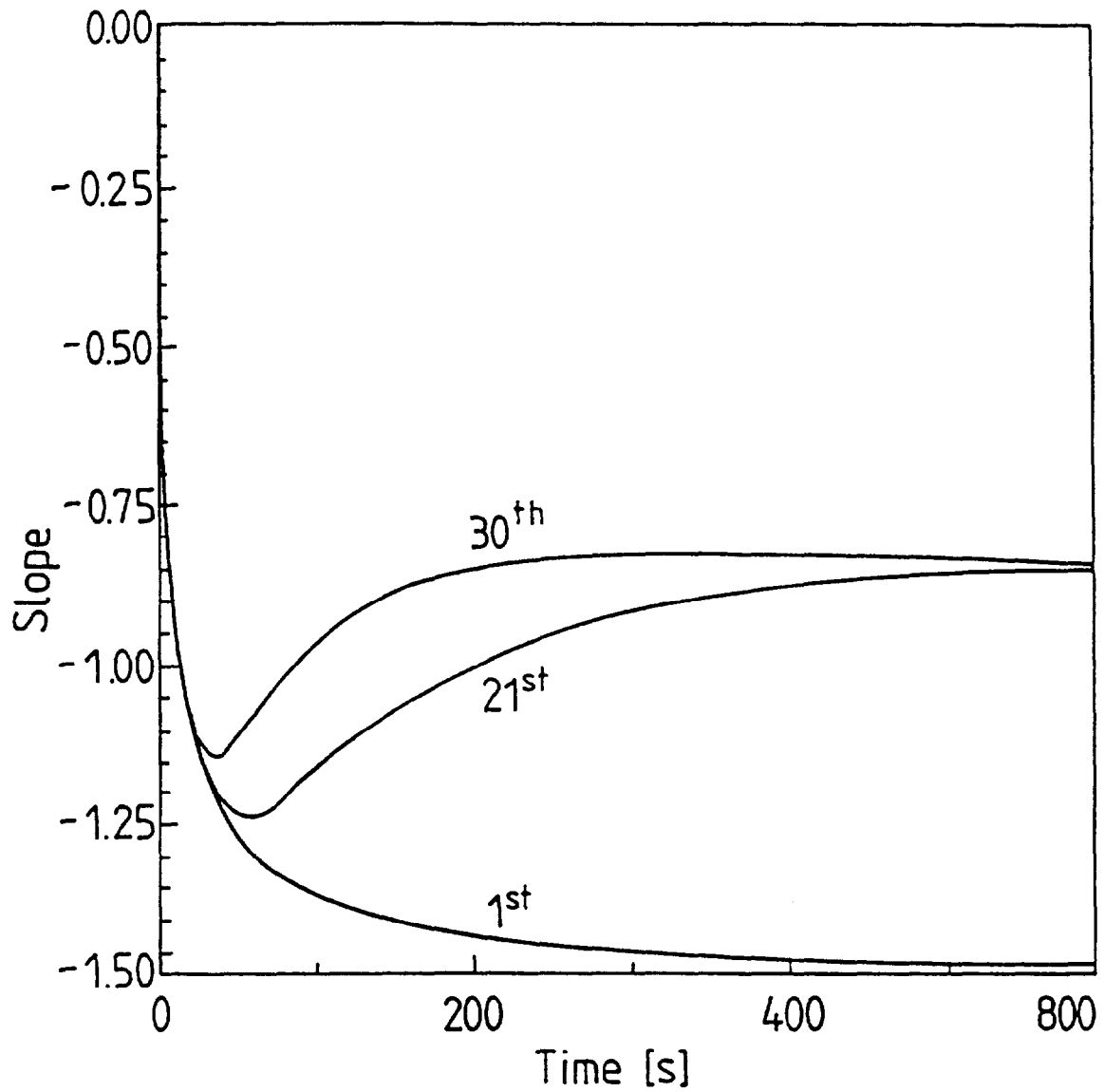


Fig 9: Calculated slopes of the logarithms of the outgassing rates versus logarithm of time after successive plasma loadings with outgassing allowed for 600 sec between shots for a DD controlled release process with  $D = 10^{-17} \text{ m}^2/\text{sec}$  and  $R = 5\text{nm}$ .

## ANNEX

P.-H. REBUT, A. GIBSON, M. HUGUET, J.M. ADAMS<sup>1</sup>, B. ALPER, H. ALTMANN, A. ANDERSEN<sup>2</sup>, P. ANDREW<sup>3</sup>, M. ANGELONE<sup>4</sup>, S. ALI-ARSHAD, P. BAIGGER, W. BAILEY, B. BALET, P. BARABASCHI, P. BARKER, R. BARNSLEY<sup>5</sup>, M. BARONIAN, D.V. BARTLETT, L. BAYLOR<sup>6</sup>, A.C. BELL, G. BENALI, P. BERTOLDI, E. BERTOLINI, V. BHATNAGAR, A.J. BICKLEY, D. BINDER, H. BINDSLEV<sup>2</sup>, T. BONICELLI, S.J. BOOTH, G. BOSIA, M. BOTMAN, D. BOUCHER, P. BOUCQUEY, P. BREGER, H. BRELEN, H. BRINKSCHULTE, D. BROOKS, A. BROWN, T. BROWN, M. BRUSATI, S. BRYAN, J. BRZOZOWSKI<sup>7</sup>, R. BUCHSE<sup>22</sup>, T. BUDD, M. BURES, T. BUSINARO, P. BUTCHER, H. BUTTGEREIT, C. CALDWELL-NICHOLS, D.J. CAMPBELL, P. CARD, G. CELENTANO, C.D. CHALLIS, A.V. CHANKIN<sup>8</sup>, A. CHERUBINI, D. CHIRON, J. CHRISTIANSEN, P. CHUILON, R. CLAESEN, S. CLEMENT, E. CLIPSHAM, J.P. COAD, I.H. COFFEY<sup>9</sup>, A. COLTON, M. COMISKEY<sup>10</sup>, S. CONROY, M. COOKE, D. COOPER, S. COOPER, J.G. CORDEY, W. CORE, G. CORRIGAN, S. CORTI, A.E. COSTLEY, G. COTTRELL, M. COX<sup>11</sup>, P. CRIPWELL<sup>12</sup>, O. Da COSTA, J. DAVIES, N. DAVIES, H. de BLANK, H. de ESCH, L. de KOCK, E. DEKSNIS, F. DELVART, G.B. DENNE-HINNOV, G. DESCHAMPS, W.J. DICKSON<sup>13</sup>, K.J. DIETZ, S.L. DMITRENKO, M. DMITRIEVA<sup>14</sup>, J. DOBBING, A. DOGLIO, N. DOLGETTA, S.E. DORLING, P.G. DOYLE, D.F. DÜCHS, H. DUQUENOY, A. EDWARDS, J. EHRENBERG, A. EKEDAHL, T. ELEVANT<sup>7</sup>, S.K. ERENTS<sup>11</sup>, L.G. ERIKSSON, H. FAJEMIROKUN<sup>12</sup>, H. FALTER, J. FREILING<sup>15</sup>, F. FREVILLE, C. FROGER, P. FROISSARD, K. FULLARD, M. GADEBERG, A. GALETSAS, T. GALLAGHER, D. GAMBIER, M. GARRIBBA, P. GAZE, R. GIANNELLA, R.D. GILL, A. GIRARD, A. GONDHALEKAR, D. GOODALL<sup>11</sup>, C. GORMEZANO, N.A. GOTTARDI, C. GOWERS, B.J. GREEN, B. GRIEVSON, R. HAANGE, A. HAIGH, C.J. HANCOCK, P.J. HARBOUR, T. HARTRAMPF, N.C. HAWKES<sup>11</sup>, P. HAYNES<sup>11</sup>, J.L. HEMMERICH, T. HENDER<sup>11</sup>, J. HOEKZEMA, D. HOLLAND, M. HONE, L. HORTON, J. HOW, M. HUART, I. HUGHES, T.P. HUGHES<sup>10</sup>, M. HUGON, Y. HUO<sup>16</sup>, K. IDA<sup>17</sup>, B. INGRAM, M. IRVING, J. JACQUINOT, H. JAECKEL, J.F. JAEGER, G. JANESCHITZ, Z. JANKOVICZ<sup>18</sup>, O.N. JARVIS, F. JENSEN, E.M. JONES, H.D. JONES, L.P.D.F. JONES, S. JONES<sup>19</sup>, T.T.C. JONES, J.-F. JUNGER, F. JUNIQUE, A. KAYE, B.E. KEEN, M. KEILHACKER, G.J. KELLY, W. KERNER, A. KHUDOLEEV<sup>21</sup>, R. KONIG, A. KONSTANTELLOS, M. KOVANEN<sup>20</sup>, G. KRAMER<sup>15</sup>, P. KUPSCHUS, R. LÄSSER, J.R. LAST, B. LAUNDY, L. LAURO-TARONI, M. LAVEYRY, K. LAWSON<sup>11</sup>, M. LENNHOLM, J. LINGERTAT<sup>22</sup>, R.N. LITUNOVSKI, A. LOARTE, R. LOBEL, P. LOMAS, M. LOUGHLIN, C. LOWRY, J. LUPO, A.C. MAAS<sup>15</sup>, J. MACHUZAK<sup>19</sup>, B. MACKLIN, G. MADDISON<sup>11</sup>, C.F. MAGGI<sup>23</sup>, G. MAGYAR, W. MANDL<sup>22</sup>, V. MARCHESE, G. MARCON, F. MARCUS, J. MART, D. MARTIN, E. MARTIN, R. MARTIN-SOLIS<sup>24</sup>, P. MASSMANN, G. MATTHEWS, H. McBRYAN, G. McCRACKEN<sup>11</sup>, J. McKIVITT, P. MERIGUET, P. MIELE, A. MILLER, J. MILLS, S.F. MILLS, P. MILLWARD, P. MILVERTON, E. MINARDI<sup>4</sup>, R. MOHANTI<sup>25</sup>, P.L. MONDINO, D. MONTGOMERY<sup>26</sup>, A. MONTVAI<sup>27</sup>, P. MORGAN, H. MORSI, D. MUIR, G. MURPHY, R. MYRNÄS<sup>28</sup>, F. NAVE<sup>29</sup>, G. NEWBERT, M. NEWMAN, P. NIELSEN, P. NOLL, W. OBERT, D. O'BRIEN, J. ORCHARD, J. O'ROURKE, R. OSTROM, M. OTTAVIANI, M. PAIN, F. PAOLETTI, S. PAPASTERGIOU, W. PARSONS, D. PASINI, D. PATEL, A. PEACOCK, N. PEACOCK<sup>11</sup>, R.J.M. PEARCE, D. PEARSON<sup>12</sup>, J.F. PENG<sup>16</sup>, R. PEPE DE SILVA, G. PERINIC, C. PERRY, M. PETROV<sup>21</sup>, M.A. PICK, J. PLANCOULAINE, J.-P. POFFÉ, R. PÖHLCHEN, F. PORCELLI, L. PORTE<sup>13</sup>, R. PRENTICE, S. PUPPIN, S. PUTVINSKII<sup>8</sup>, G. RADFORD<sup>30</sup>, T. RAIMONDI, M.C. RAMOS DE ANDRADE, R. REICHLER, J. REID, S. RICHARDS, E. RIGHI, F. RIMINI, D. ROBINSON<sup>11</sup>, A. ROLFE, R.T. ROSS, L. ROSSI, R. RUSS, P. RUTTER, H.C. SACK, G. SADLER, G. SAIBENE, J.L. SALANAVE, G. SANAZZARO, A. SANTAGIUSTINA, R. SARTORI, C. SBORCHIA, P. SCHILD, M. SCHMID, G. SCHMIDT<sup>31</sup>, B. SCHUNKE, S.M. SCOTT, L. SERIO, A. SIBLEY, R. SIMONINI, A.C.C. SIPS, P. SMEULDERS, R. SMITH, R. STAGG, M. STAMP, P. STANGEBY<sup>3</sup>, R. STANKIEWICZ<sup>32</sup>, D.F. START, C.A. STEED, D. STORK, P.E. STOTT, P. STUBBERFIELD, D. SUMMERS, H. SUMMERS<sup>13</sup>, L. SVENSSON, J.A. TAGLE<sup>33</sup>, M. TALBOT, A. TANGA, A. TARONI, C. TERELLA, A. TERRINGTON, A. TESINI, P.R. THOMAS, E. THOMPSON, K. THOMSEN, F. TIBONE, A. TISCORNIA, P. TREVALION, B. TUBBING, P. VAN BELLE, H. VAN DER BEKEN, G. VLASES, M. VON HELLERMANN, T. WADE, C. WALKER, R. WALTON<sup>31</sup>, D. WARD, M.L. WATKINS, N. WATKINS, M.J. WATSON, S. WEBER<sup>34</sup>, J. WESSON, T.J. WIJNANDS, J. WILKS, D. WILSON, T. WINKEL, R. WOLF, D. WONG, C. WOODWARD, Y. WU<sup>35</sup>, M. WYKES, D. YOUNG, I.D. YOUNG, L. ZANNELLI, A. ZOLFAGHARI<sup>19</sup>, W. ZWINGMANN

- 
- <sup>1</sup> Harwell Laboratory, UKAEA, Harwell, Didcot, Oxfordshire, UK.
  - <sup>2</sup> Risø National Laboratory, Roskilde, Denmark.
  - <sup>3</sup> Institute for Aerospace Studies, University of Toronto, Downsview, Ontario, Canada.
  - <sup>4</sup> ENEA Frascati Energy Research Centre, Frascati, Rome, Italy.
  - <sup>5</sup> University of Leicester, Leicester, UK.
  - <sup>6</sup> Oak Ridge National Laboratory, Oak Ridge, TN, USA.
  - <sup>7</sup> Royal Institute of Technology, Stockholm, Sweden.
  - <sup>8</sup> I.V. Kurchatov Institute of Atomic Energy, Moscow, Russian Federation.
  - <sup>9</sup> Queens University, Belfast, UK.
  - <sup>10</sup> University of Essex, Colchester, UK.
  - <sup>11</sup> Culham Laboratory, UKAEA, Abingdon, Oxfordshire, UK.
  - <sup>12</sup> Imperial College of Science, Technology and Medicine, University of London, London, UK.
  - <sup>13</sup> University of Strathclyde, Glasgow, UK.
  - <sup>14</sup> Keldysh Institute of Applied Mathematics, Moscow, Russian Federation.
  - <sup>15</sup> FOM-Institute for Plasma Physics "Rijnhuizen", Nieuwegein, Netherlands.
  - <sup>16</sup> Institute of Plasma Physics, Academia Sinica, Hefei, Anhui Province, China.
  - <sup>17</sup> National Institute for Fusion Science, Nagoya, Japan.
  - <sup>18</sup> Soltan Institute for Nuclear Studies, Otwock/Świerk, Poland.
  - <sup>19</sup> Plasma Fusion Center, Massachusetts Institute of Technology, Boston, MA, USA.
  - <sup>20</sup> Nuclear Engineering Laboratory, Lappeenranta University, Finland.
  - <sup>21</sup> A.F. Ioffe Physico-Technical Institute, St. Petersburg, Russian Federation.
  - <sup>22</sup> Max-Planck-Institut für Plasmaphysik, Garching, Germany.
  - <sup>23</sup> Department of Physics, University of Milan, Milan, Italy.
  - <sup>24</sup> Universidad Complutense de Madrid, Madrid, Spain.
  - <sup>25</sup> North Carolina State University, Raleigh, NC, USA.
  - <sup>26</sup> Dartmouth College, Hanover, NH, USA.
  - <sup>27</sup> Central Research Institute for Physics, Budapest, Hungary.
  - <sup>28</sup> University of Lund, Lund, Sweden.
  - <sup>29</sup> Laboratório Nacional de Engenharia e Tecnologia Industrial, Sacavem, Portugal.
  - <sup>30</sup> Institute of Mathematics, University of Oxford, Oxford, UK.
  - <sup>31</sup> Princeton Plasma Physics Laboratory, Princeton University, Princeton, NJ, USA.
  - <sup>32</sup> RCC Cyfronet, Otwock/Świerk, Poland.
  - <sup>33</sup> Centro de Investigaciones Energéticas, Medioambientales y Tecnológicas, Madrid, Spain.
  - <sup>34</sup> Freie Universität, Berlin, Germany.
  - <sup>35</sup> Institute for Mechanics, Academia Sinica, Beijing, China.